Refinement of Objective Motion Cueing Criteria Based on Three Flight Tasks

Peter M.T. Zaal*
San Jose State University
NASA Ames Research Center
Moffett Field, CA

Jeffery A. Schroeder†
Federal Aviation Administration
Moffett Field, CA

William W. Chung‡
Science Applications International Corporation
NASA Ames Research Center
Moffett Field, CA

This paper aims to refine objective motion cueing criteria developed in a previous experiment for the simulator motion system diagnostic test specified by the International Civil Aviation Organization. Fifteen airline transport pilots flew the same three tasks as in the previous experiment in the NASA Vertical Motion Simulator under six different motion configurations. The six different motion configurations covered the motion region between the motion fidelity uncertainty boundary found in the previous experiment and the mean motion response of a statistical sample of eight representative hexapod motion simulators. The motion condition significantly affected 1) roll deviations in the approach to a stall and maximum pitch rate in a stall recovery, and 2) heading deviation and pedal reaction time after an engine failure in the takeoff task. Significant differences in pilot-vehicle performance were used to develop new objective motion cueing criteria boundaries for the main motion responses. In addition, perception thresholds of false motion cues were used to develop motion cueing criteria for the cross-coupling motion responses. The fidelity boundaries of the current experiment should be used with caution when reducing the uncertainty of the initial fidelity boundaries developed in the previous experiment, as they do not fully overlap. Data collected in the current study will add to data from the next experiment, which aims to further refine and optimize the objective motion criteria found to date.

Nomenclature

AFS	analogue fidelity scale, %
fx, fy, fz	surge, sway, heave specific force, ft/s^2
g	gravitational acceleration, ft/s^2
H	OMCT frequency response
$\dot{h}_{td}$	sink rate of main gear at touchdown, ft/s
N_1	engine fan speed, %
N_s	number of stick shakers
p, q, r	roll, pitch, yaw rate, deg/s
q_{max}	maximum pitch rate, rad/s
RMS_{gs}	RMS of glideslope deviation, dot
RMS_V	RMS of indicated airspeed deviation, kts
RMS_ϕ	RMS of roll deviation, deg
RMS_ψ	RMS of heading deviation, deg
t_p	pedal-response time, s
V_2	takeoff safety speed, kts
V_r	rotation speed, kts
V_{ref}	reference speed, kts
x, y, z	surge, sway, heave
Δx_{td}	longitudinal touchdown deviation of main gear, ft
Δy_{td}	lateral touchdown deviation of main gear, ft
ω	frequency , rad/s

Abbreviations

CAVU	ceiling and visibility unlimited
FL	flight level
GS	glideslope
LOC	localizer
OMCT	Objective Motion Cueing Test
RMS	root mean square
RWY	runway
VMS	Vertical Motion Simulator

*Research Associate, Human Systems Integration Division, NASA Ames Research Center, Moffett Field, CA, 94035; peter.m.t.zaal@nasa.gov. Member.

†Chief Scientific and Technical Advisor for Flight Simulation Systems, Federal Aviation Administration, Moffett Field, CA, 94035; jeffery.schroeder@faa.gov. Associate Fellow.

‡Simulation Engineer, Simulation Laboratories, NASA Ames Research Center, Moffett Field, CA, 94035; william.w.chung@nasa.gov. Senior Member.

I. Introduction

The objective of this paper is to refine objective motion cueing criteria for commercial transport simulators based on pilots' performance in three flying tasks. Actuator hardware and software algorithms determine motion cues. Today, during a simulator qualification, engineers objectively evaluate only the hardware.[1] Pilot inspectors subjectively assess the overall motion cueing system (i.e., hardware plus software); however, it is acknowledged that pinpointing any deficiencies that might arise to either hardware or software is challenging. ICAO 9625 has an Objective Motion Cueing Test (OMCT), which is now a required test in the FAAs part 60 regulations for new devices, evaluating the software and hardware together; however, it lacks accompanying fidelity criteria.[1,2] Hosman has documented OMCT results for a statistical sample of eight simulators,[3] which is useful, but having validated criteria would be an improvement. In a previous experiment, we developed initial objective motion cueing criteria that this paper is trying to refine.

Sinacori suggested simple criteria,[4,5] which are in reasonable agreement with much of the literature.[6–15] These criteria often necessitate motion displacements greater than most training simulators can provide. While some of the previous work has used transport aircraft in their studies, the majority used fighter aircraft or helicopters.[6–11] Those that used transport aircraft considered degraded flight characteristics.[12–15] As a result, earlier criteria lean more towards being sufficient, rather than necessary, criteria for typical transport aircraft training applications. Considering the prevalence of 60-inch, six-legged hexapod training simulators, a relevant question is "what are the necessary criteria that can be used with the ICAO 9625 diagnostic?"

This study adds to the literature as follows. First, it examines well-behaved transport aircraft characteristics, but in three challenging tasks. The tasks are equivalent to the ones used in our previous experiment, allowing us to directly compare the results and add to the previous data. Second, it uses the Vertical Motion Simulator (VMS), the world's largest vertical displacement simulator. This allows inclusion of relatively large motion conditions, much larger than a typical training simulator can provide. Six new motion configurations were used that explore the motion responses between the initial objective motion cueing boundaries found in a previous experiment and what current hexapod simulators typically provide. Finally, a sufficiently large pilot pool added statistical reliability to the results.

II. Flight Tasks

The goal of the current study was to refine the objective motion cueing criteria based on pilots' performance in three flight tasks developed in the previous study, discussed in Ref. 16. For this reason, the current study had the same three flight tasks as the previous study with some minor improvements: an approach and landing with sidestep maneuver, a high-altitude stall recovery, and an engine-out after takeoff. The assumption was that varying the motion cues would affect how pilots perform these challenging tasks. Fig. 1 shows the flight cards for the three tasks, which the following sections describe.

II.A. Approach and Landing with Sidestep

This task began at an altitude of 1,250 ft on a -3 deg glideslope approach to RWY 28R at San Francisco International Airport. Moderate turbulence, simulated using the Dryden turbulence model, existed throughout.[17] After breaking out of the cloud ceiling at 1,100 ft, air traffic control instructed the pilots to sidestep to RWY 28L. Pilots tried to maintain a -3 deg glideslope during the approach followed by landing within a 750-ft-long and 28-ft-wide box with a sink rate of 6 ft/s or less. An audio call-out began at a main gear height of fifty feet and repeated in decrements of 10 ft until touchdown. An overview of the runway configuration and definition of the touchdown box is given in Fig. 2.

This task evaluated if changes in motion cues affect 1) lateral-directional control in the sidestep maneuver, 2) speed and flightpath control along the glideslope, and 3) touchdown performance.

II.B. High Altitude Stall Recovery

The task started during cruise at 210 kts ($M = 0.75$) at an altitude of 41,000 ft. Pilots were instructed to initiate a self-induced stall by setting the throttles to idle, rolling 20 degs left and pitching approximately 15 degs nose up, decelerating through the stall warning until a negative sink rate was developed (as the aircraft model did not have a pronounced pitch break). To recover from the stall, pilots had to follow the correct recovery sequence of reducing the angle-of-attack (by pitching to approximately 15 deg nose down), leveling the wings, and applying full throttle until establishing a safe positive climb rate. The task called for the pilots to pull the nose up gently and smoothly so as not to activate the stall warning during the recovery. Moderate turbulence was present.

Task: approach to SFO RWY 28R with sidestep to landing on RWY 28L

Initial Condition: 1,250 ft altitude at V_{ref}+5 on GS and LOC for 28R

Configuration: gear down, flaps 30 deg

Ceiling/visibility: 1,100 ft ceiling, 10-mile visibility

Wind: 230/15 **Turbulence:** moderate **Gusts:** none

Procedure:

1. Track the GS and LOC to SFO RWY 28R maintaining 141 KIAS
2. Perform sidestep to RWY 28L at ATC command
3. Continue visual to RWY 28L maintaining GS
4. Flare and touchdown 750 –1,500 ft from the threshold

Desired performance:

1. Deviation from 141 KIAS within $\pm$5 kts until 200 ft altitude
2. Glideslope deviation within $\pm$ one dot until 200 ft altitude
3. Longitudinal touchdown 750 –1,500 ft from threshold
4. Lateral touchdown $\pm$14 ft from centreline
5. Sink rate at touchdown $\leq$6 ft/s

(a) Approach and landing with sidestep

Task: recover from a high altitude stall

Initial Condition: level at FL 410 and 210 KIAS

Configuration: clean

Ceiling/visibility: CAVU

Wind: none **Turbulence:** moderate **Gusts:** none

Procedure:

1. Retard throttle to idle
2. Roll left to a 20 deg bank angle
3. Pull up to decelerate at approximately 4 kt/s
4. Continue deceleration through stick shaker until a sink rate develops
5. Apply nose down pitch, roll as needed, power as needed to return to steady-state flight

Desired performance:

1. Maintain bank angle within $\pm$5 degs about 15 degs during entry
2. Proper stall recovery procedure (push, roll, thrust, stabilized flight)
3. Recovers smoothly to speed $>$210 KIAS and positive rate of climb
4. Recover without exceeding airplane's limitations
5. Oscillatory load factor peaks between 0.75 and 1.25 g
6. During recovery, no more than one additional stick shaker activation

(b) High altitude stall recovery

Task: recover from engine out on takeoff

Initial Condition: at takeoff position on RWY 28R

Configuration: gear down, flaps 10 deg

Ceiling/visibility: CAVU

Wind: none **Turbulence:** none **Gusts:** none

Procedure:

1. Advance throttles to takeoff thrust (90% N_1)
2. Maintain centreline
3. Rotate at V_r=128 kts, pitch to 10 degs and establish speed of V_2+10
4. Maintain heading and speed after single engine failure

Desired performance:

1. Desired heading $\pm$5 degs
2. Desired airspeed $\pm$5 kts
3. Bank approximately 5 degs towards operating engine

(c) Engine out after takeoff

Figure 1. Experiment flight cards.

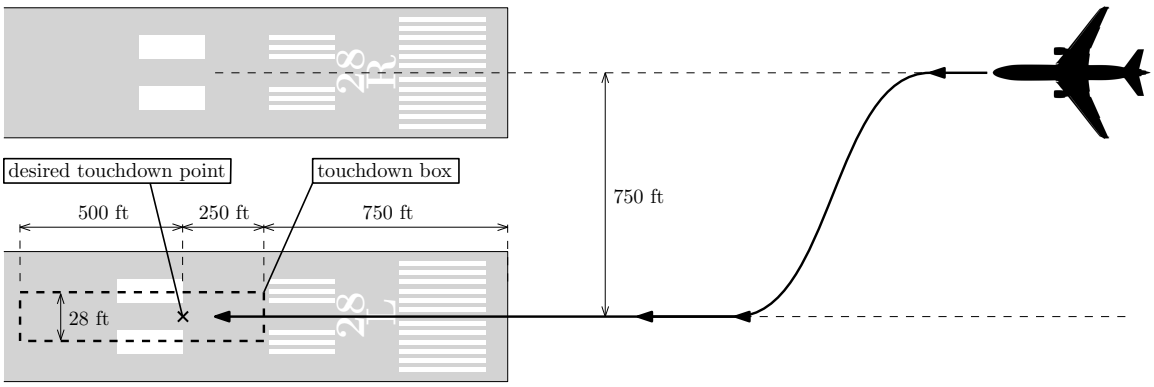

Figure 2. Runway configuration and touchdown box definition.

This task evaluated if changes in motion cues affect the recovery performance by helping a pilot damp the flight path response, as well as stabilize the progressively less-stable roll dynamics near stall.

II.C. Engine Out after Takeoff

During the takeoff roll, the task required pilots to rotate at 128 kts, establish a 10 deg nose up pitch attitude, and maintain a steady climb speed of 145 kts. Either the left or right engine failed randomly at a random altitude after liftoff but below 100 ft. After identifying the failed engine, pilots needed to apply near full rudder pedal towards the good engine, roll approximately 5 deg into the direction of the good engine to maintain the desired track, and modulate the remaining thrust to maintain speed.

This task evaluated if changes in motion cues affect a pilot's ability to detect the failed engine promptly and recover using appropriate lateral-directional control.

II.D. Aircraft Model

The experimenters modified an existing mid-size twin-engine commercial transport aircraft model with a gross weight of 185,800 lbs for this study. The enhancements allowed for a more representative aircraft response in the stall task. Most significantly, modifications to the lift coefficient as a function of angle of attack allowed for typical transport post-stall characteristics. Modifications to the rolling moment coefficient due to roll rate allowed for satisfactory representation of reduced roll stability near stall. Finally, modifications to the rolling moment coefficient due to aileron inputs allowed for an adequate representation of reduced roll control authority near the stall.

The simulated aircraft had six degrees of freedom and a two-crew cockpit. The aircraft model included a landing gear model, allowing it to taxi, takeoff, and land. The aircraft could operate in the typical transport envelope up to a maximum cruising altitude of 42,000 ft.

III. Motion Configurations

Pilots performed each flight task with the same six motion configurations. Only the motion parameters of the roll and heave degrees of freedom for the stall task were slightly different from the landing and takeoff tasks to accommodate the large roll and vertical excursions during the stall. The experiment used the standard VMS motion algorithm and hardware for all motion configurations. The equivalent time delays of the VMS motion system for the pitch, roll, yaw, longitudinal, lateral, and vertical axes are 47, 68, 48, 50, 69, and 67 ms, respectively. More details about the VMS motion system are provided in Ref. 18. In the remainder of this paper, the four motion configurations of the previous study, referred to as MCUE2014, are labeled by M1-M4. The six motion configurations of the current study, referred to as MCUE2015, are labeled by M5-M10 (Table 1).

Table 1. Motion configurations.

experiment	label	motion
MCUE2014 (Ref. 16)	M1	large VMS motion (LMOT)
	M2	low-gain/low-break-frequency hexapod motion (HEX-L)
	M3	medium-gain/medium-break-frequency hexapod motion (HEX-M)
	M4	high-gain/high-break-frequency hexapod motion (HEX-H)
MCUE2015	M5	mean OMCT + σ (defined in Ref. 3)
	M6	mean OMCT
	M7	mean OMCT + $1/3\ \Delta_1$
	M8	mean OMCT + $2/3\ \Delta_1$
	M9	lower fidelity boundary edge (defined in Ref. 16)
	M10	lower fidelity boundary edge + $1/4\ \Delta_2$

The six motion configurations of the current study were selected to encompass the lower edge of the objective motion cueing criteria fidelity boundaries developed in the previous study[16] and the means of the Objective Motion Cueing Test (OMCT) responses from a statistical sample of eight simulators.[3] Fig. 3 details the selection of the six motion configurations using the magnitude of the OMCT motion response for any degree of freedom. The mean OMCT responses plus one standard deviation and the mean OMCT responses were the first two motion configurations (M5 and M6, respectively). A simulation model of the VMS motion logic was used to calculate the motion parameters

of M5 and M6 by fitting their simulated OMCT responses to the mean-OMCT and mean-OMCT-plus-one-standard-deviation responses. The lower edge of the initial objective motion cueing criteria fidelity boundaries determined in Ref. 16 was used to determine a third motion configuration M9. The difference between the lower boundary edge and the mean OMCT responses, Δ_1, was used to determine M7 and M8. The motion parameters of these two configurations and M6 and M9 were equally spaced $\frac{1}{3}\Delta_1$ from each other (Fig. 3). For the final motion configuration M10, the difference between the lower and upper boundary edges of the initial objective motion cueing criteria fidelity boundaries, Δ_2, was used. The motion parameters of M10 were defined by the lower boundary plus $\frac{1}{4}\Delta_2$.

Fig. 3 provides a schematic overview of the method used to define the motion configurations, and only shows the variation in motion gain. In reality, the method also extended to the other motion parameters, such as the washout break frequencies and damping ratios. In addition, the uncertainty boundaries of the initial objective motion cueing criteria and the area defined by the means plus and minus one standard deviation of the OMCT responses overlaped. Fig. 4 depicts the calculated OMCT responses for the roll degree of freedom of the motion configurations for the sidestep task. The motion tuning approach followed is especially clear at higher frequencies in the magnitude plot and in the phase plot. Fig. 4 shows that the six motion configurations of the current study span the area between the lower criteria uncertainty boundaries and the mean plus one standard deviation of the OMCT response; that is, the area of the OMCT fidelity region associated with lower fidelity motion. This area was not fully covered in the previous experiment.[16] Note that the OMCT responses in Fig. 4 are not from actual measurements and motion system dynamics are not included.

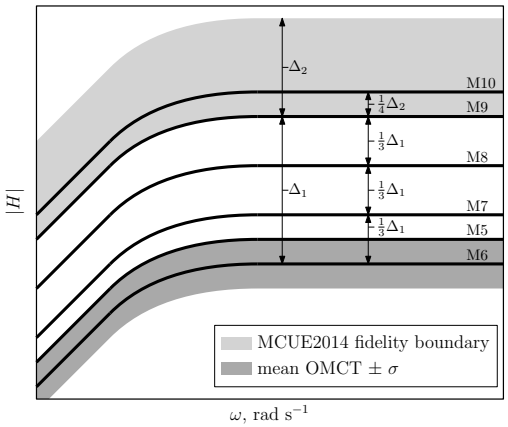

Figure 3. Motion configuration definition.

In the previous experiment, three of the four motion configurations were tuned to fit on a hexapod motion system with 60-inch legs (M2-M4). To that extent, a hexapod algorithm was implemented to run in parallel with the VMS motion logic for motion tuning and monitoring purposes.[16] In the current experiment, no emphasis was placed on developing specific hexapod motion configurations. However, due to the nature of their definition, motion configurations M5 to M9 mostly remained within the hexapod motion envelope for all three tasks.

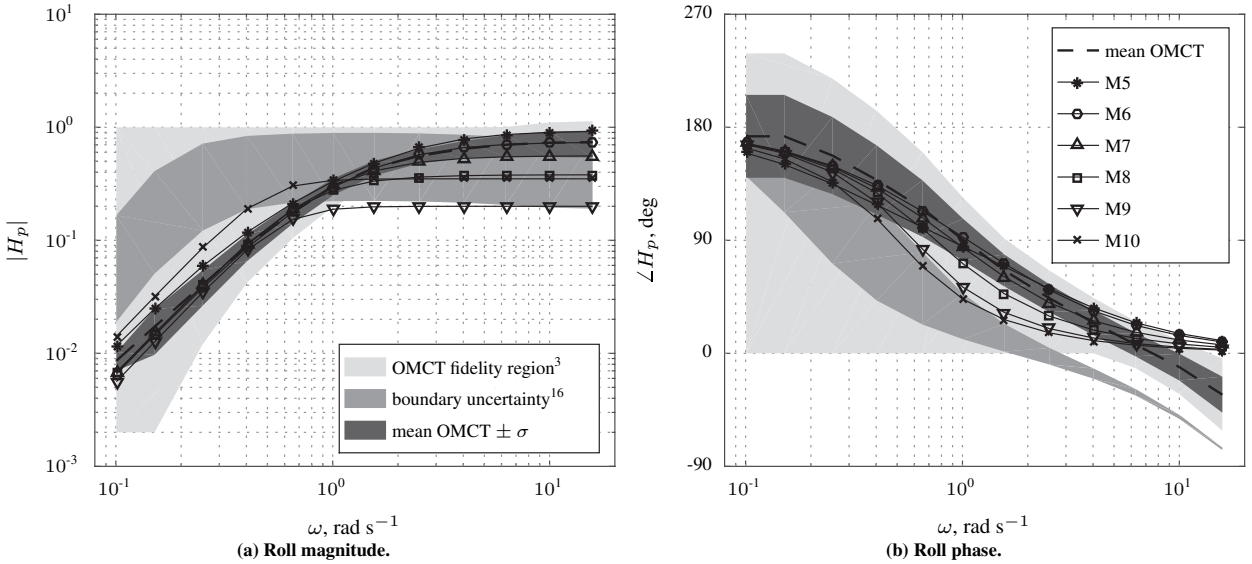

(a) Roll magnitude. **(b) Roll phase.**

Figure 4. Calculated roll OMCT responses of the sidestep task motion configurations.

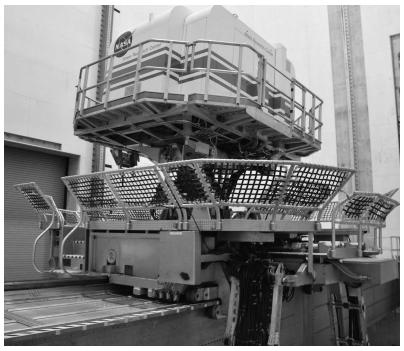

Figure 5. Vertical Motion Simulator.

Figure 6. Cockpit setup.

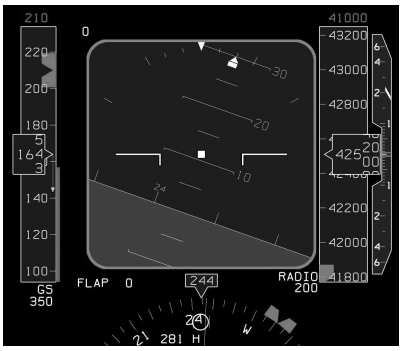

Figure 7. Primary flight display.

IV. Experiment Setup

IV.A. Independent Variable

Motion configuration was the only independent variable, with six levels (M5-M10). Every pilot flew each task with all six motion configurations (Table 1).

IV.B. Apparatus

The experiment used the VMS with the transport cab (T-CAB) (Fig. 5).[18] Pilots flew from the left seat; the instructor occupied the right seat. A primary flight display (PFD) was positioned in front of each pilot (Fig. 6). The navigation displays were positioned next to the PFDs towards the center of the cab. An additional display in the center of the cab showed the engine parameters. This display changed to show task performance after each run.

A column and wheel controlled aircraft pitch and roll, respectively. A thumb switch on the wheel controlled elevator trim. Conventional rudder pedals controlled the rudder deflection in the air and nose wheel steering on the ground. Two throttle levers controlled the power of the two engines. The instructor pilot configured flaps and gear with representative controls before each task.

The PFD symbology was similar to that on a Boeing 777 (Fig. 7). Speed and heading bugs indicated the desired speed and heading for each task. In addition, typical symbology on the speed tape indicated the minimum and maximum speeds, and V-speeds. The PFD also depicted conventional localizer and glide slope error indicators. A green speed trend vector originating from the indicated airspeed showed what the airspeed would be in 10 s. The control columns in the cockpit had stick shakers to warn pilots of an impending stall. The activation of the shakers occurred simultaneously when the minimum speed tape, also known as the "barber pole", coincided with the indicated airspeed.

The collimated out-the-window display of T-CAB consisted of a projection system projecting a high-quality image on six spherical mirrors. The mirrors formed a dome-like section providing a continuous field-of-view image to both pilots. The out-the-window visual had a 220° horizontal field of view and a 28° vertical field of view (10° up and 18° down). A Rockwell-Collins EPX5000 computer image generator created the out-the-window visual scene. The visual system equivalent time delay was 62 ms.[18] This was in line with the equivalent time delays of the motion system (Section III).

A Microsoft® Surface™ tablet was used by pilots to provide motion ratings.

IV.C. Procedures

The pilot pre-briefing explained the purpose of the experiment, the procedures, conditions, and performance criteria for each flight task. Pilots were informed they would perform each task with six different motion configurations and that the configurations would be presented randomly. However, no specifics about the motion configurations were given.

Pilots performed all three tasks, each with the six different motion configurations. Each motion configuration was repeated six times for a total of 36 runs per task. The first six runs were used as training runs in which the six motion conditions were presented once each. The remaining 30 runs were used for data analysis. The tasks and motion configurations were presented randomly. A randomized Latin square determined the order of the tasks and

motion configurations. All runs for a particular task were performed in a single session. Each task session lasted one-and-a-half to two hours, and breaks were taken in between sessions.

Before each task, the instructor pilot reviewed the procedures, performance criteria, the relevant controls, and displays. The instructor evaluated a pilot's performance after each run using task performance information displayed in the cab. An experiment observer in the control room verified the evaluation. After completing each run, participant pilots rated the motion of two specific parts of the task with two different rating scales on a tablet PC (Section IV.E).

IV.D. Participants

Fifteen experienced airline transport pilots participated. Each pilot except one had a B757/B767 type rating, as the aircraft model used in the simulation was of an aircraft similar to a B757 in terms of configuration, size, and weight. All pilots had experience on many other aircraft types. The average number of flying hours pilots had on a B757/B767 was 4,658 with a standard deviation of $\pm$4,259. The average number of flying hours on other aircraft types was 7,969 with a standard deviation of $\pm$5,064. All pilots were male and eleven had experience as a captain. Ten out of the 12 pilots who participated in the previous experiment, discussed in Ref. 16, participated in the current experiment.

IV.E. Dependent Measures

Six subjective dependent measures and 11 objective dependent measures were recorded and analyzed. Pilots rated the simulator motion of two specific parts of each task with two different ratings in each run. For each rating, pilots answered a question by moving a digital slider on an analogue fidelity scale (AFS). The analogue scale ranged from 0% (low fidelity) to 100% (high fidelity). The following questions were asked for the sidestep task:

1. How would you rate motion fidelity in the sidestep turns with respect to what you would expect from real flight?
2. How would you rate motion fidelity in the landing flare with respect to what you would expect from real flight?

the stall task:

1. How would you rate motion fidelity in the approach to the stall with what you would expect from real flight?
2. How would you rate motion fidelity in the stall recovery with what you would expect from real flight?

and the takeoff task:

1. How would you rate motion fidelity in the initial takeoff roll with respect to what you would expect from real flight?
2. How would you rate motion fidelity right after the engine failure with respect to what you would expect from real flight?

Several objective measures determined the effect of motion on task performance. Many measures related directly to the performance criteria (Fig. 1). For the approach and landing with sidestep, the RMS of the glide slope, RMS_{gs}, and speed deviation during the approach, RMS_V, were calculated. Calculations for these variables used data from the last 60 s before reaching the decision altitude of 200 ft. When the main gear touched the runway, data captures occurred for the sink rate, $\dot{h}_{td}$, and the longitudinal and lateral deviations, Δx_{td} and Δy_{td}, from the desired touchdown point.

For the stall recovery, the RMS roll error, RMS_ϕ, applied to the 30 s before the start of the stall recovery. The maximum pitch rate deviation, q_{max}, and the number of stick shakers, N_s, applied to the stall recovery segment. Pitch rate was substituted as a partial surrogate to analyze load factor oscillations in the stall recovery, as it was more suitable for analyzing oscillatory behavior. Finally, for the engine out on takeoff task, the RMS of the heading and speed deviations after the engine failure, RMS_ψ and RMS_V, used data from the last 15 s after the engine failure. The reaction time of the initial pedal input after the engine failure, t_p, was from the time of the engine failure to the time when the pedal input was 10% of the maximum input.

V. Results

This section presents the mean results of the 15 pilots for the approach and landing with sidestep, high-altitude stall recovery, and engine out after takeoff tasks. For every pilot, data from the last five runs for each task and motion configuration were averaged. Error-bar plots present the continuous-interval dependent measures, with means and 95% confidence intervals for each motion condition. Bar plots present the ordinal dependent measures, with the number of occurrences for each dependent measure level and the median for each motion condition. Wherever appropriate, grey dashed lines depict the task performance criteria. Note that this section discusses the results of the current experiment (MCUE2015) only. The results of the previous experiment (MCUE2014) are discussed in Ref. 16 and are given here for reference only.

A repeated-measures analysis of variance (ANOVA) detected possible statistically significant differences in the continuous interval dependent measures.[19] A Friedman test was used for the ordinal dependent measures. For the ANOVA to produce accurate results, the data must meet three assumptions: 1) there should be no significant outliers, 2) data should be approximately normally distributed for each level of the independent variable, and 3) variances of the differences between all combinations of levels of the independent variable must be equal (i.e., assumption of sphericity).

Box plots identified outliers, normality was checked using the Shapiro-Wilk test, and Mauchly's test checked the assumption of sphericity. Few outliers were detected, so they were kept in the data analysis. Data were generally normally distributed. In the few cases they were not, we did not correct for it, as an ANOVA is fairly robust to deviations from normality. When the assumption of sphericity was violated, the degrees of freedom of the ANOVA were corrected using the Greenhouse-Geisser adjustment.

Post-hoc tests with Bonferroni adjustment were performed for pairwise comparisons of motion conditions when the ANOVA indicated an overall significant difference. All statistical tests had a significance level of 0.05. Table 2 gives a summary of the statistical test results for all the repeated measures (Section IV.E). In this table, df are the degrees of freedom, F or χ^2 is the test statistic for the ANOVA or Friedman test, respectively, p is the probability of observing an effect, and η^2 is the partial eta-squared, indicating sample effect size.

Table 2. Summary of statistical test results.

Measure	df	F/χ^2	p	η^2	Sig.
Sidestep Task					
$AFS1$	5.0,70.0	0.285	0.920	0.020	–
$AFS2$	5.0,70.0	0.515	0.764	0.036	–
RMS_{gs}	5.0,70.0	0.304	0.909	0.021	–
RMS_V	5.0,70.0	0.430	0.826	0.030	–
$\dot{h}_{td}$	5.0,70.0	1.048	0.396	0.070	–
Δx_{td}	5.0,70.0	1.464	0.213	0.095	–
Δy_{td}	5.0,70.0	1.859	0.113	0.117	–
Stall Task					
$AFS1$	$1.5,21.6^{gg}$	1.545	0.235	0.099	–
$AFS2$	$2.6,40.0^{gg}$	1.095	0.357	0.073	–
RMS_ϕ	$3.1,43.4^{gg}$	4.948	0.004	0.261	**
q_{max}	$2.3,31.7^{gg}$	3.519	0.037	0.201	**
N_s	5.0	5.555	0.352	–	–
Takeoff Task					
$AFS1$	$1.4,19.5^{gg}$	1.886	0.185	0.119	–
$AFS2$	5.0,70.0	1.647	0.194	0.105	–
RMS_ψ	5.0,70.0	7.305	0.000	0.343	**
RMS_V	5.0,70.0	0.599	0.701	0.041	–
t_p	5.0,70.0	5.955	0.000	0.298	**

gg = Greenhouse-Geisser correction
** = significant ($p < 0.05$)
* = marginally significant ($0.05 \leq p < 0.1$)
– = not significant ($p \geq 0.1$)

Next, motion-fidelity-rating results are presented, followed by the task-performance results, and an analysis of the magnitude of false motion cues. Finally, objective motion cueing criteria resulting from the task-performance and false-motion-cue results are presented.

V.A. Motion Fidelity Ratings

Pilots rated the motion fidelity of two specific parts of each task by moving a slider on an analogue fidelity scale between 0% and 100% (Section IV.E). This resulted in ratings $AFS1$ and $AFS2$ provided in Figures 8, 9, and 10 for the sidestep, stall, and takeoff tasks, respectively. The ANOVA did not reveal any significant differences between motion conditions for any of the AFS ratings (Table 2). For the sidestep task, pilots rated the motion fidelity compared to real flight in the sidestep turns around 60% in each condition (Fig. 8a), and motion fidelity in the landing flare between 50 and 60% (Fig. 8b). For the stall task, motion in the approach to the stall and in the stall recovery was rated around 70% in each condition (Figures 9a and 9b, respectively). Finally, for the takeoff task, motion during the initial takeoff roll and after the engine failure was rated between 60 and 70% in each condition (Figures 10a and 10b, respectively).

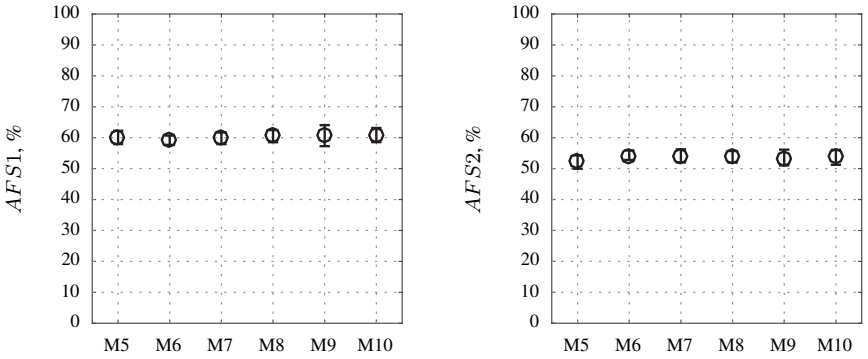

(a) Rating 1 **(b) Rating 2**

Figure 8. Motion fidelity ratings for the sidestep task.

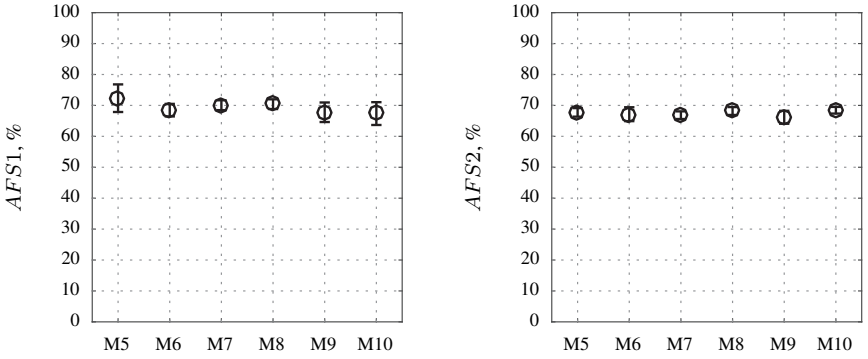

(a) Rating 1 **(b) Rating 2**

Figure 9. Motion fidelity ratings for the stall task.

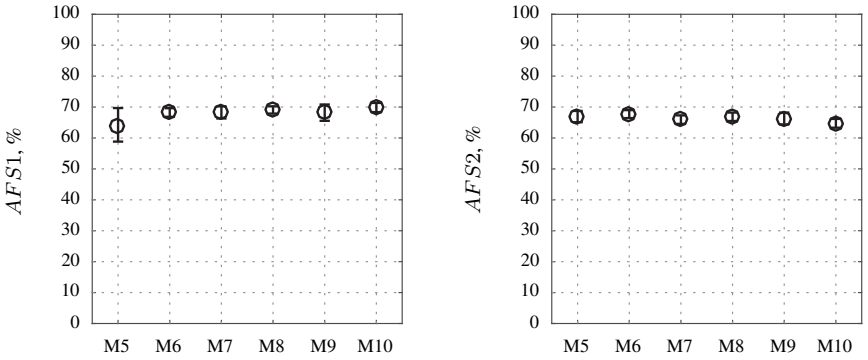

(a) Rating 1 **(b) Rating 2**

Figure 10. Motion fidelity ratings for the takeoff task.

V.B. Task Performance

V.B.1. Approach and Landing with Sidestep Task

Fig. 11 provides the task performance results for the approach and landing with sidestep task. The RMS of the glideslope and speed deviation in the approach are given in Figures 11a and 11b, respectively. No significant differences were found between conditions for both variables (Table 2). Note that pilots were able to meet the glideslope-deviation performance requirement easily with an average glideslope deviation of around 0.4 dots. Results were very similar to the previous experiment. Pilots had difficulties meeting the speed-deviation performance requirement with

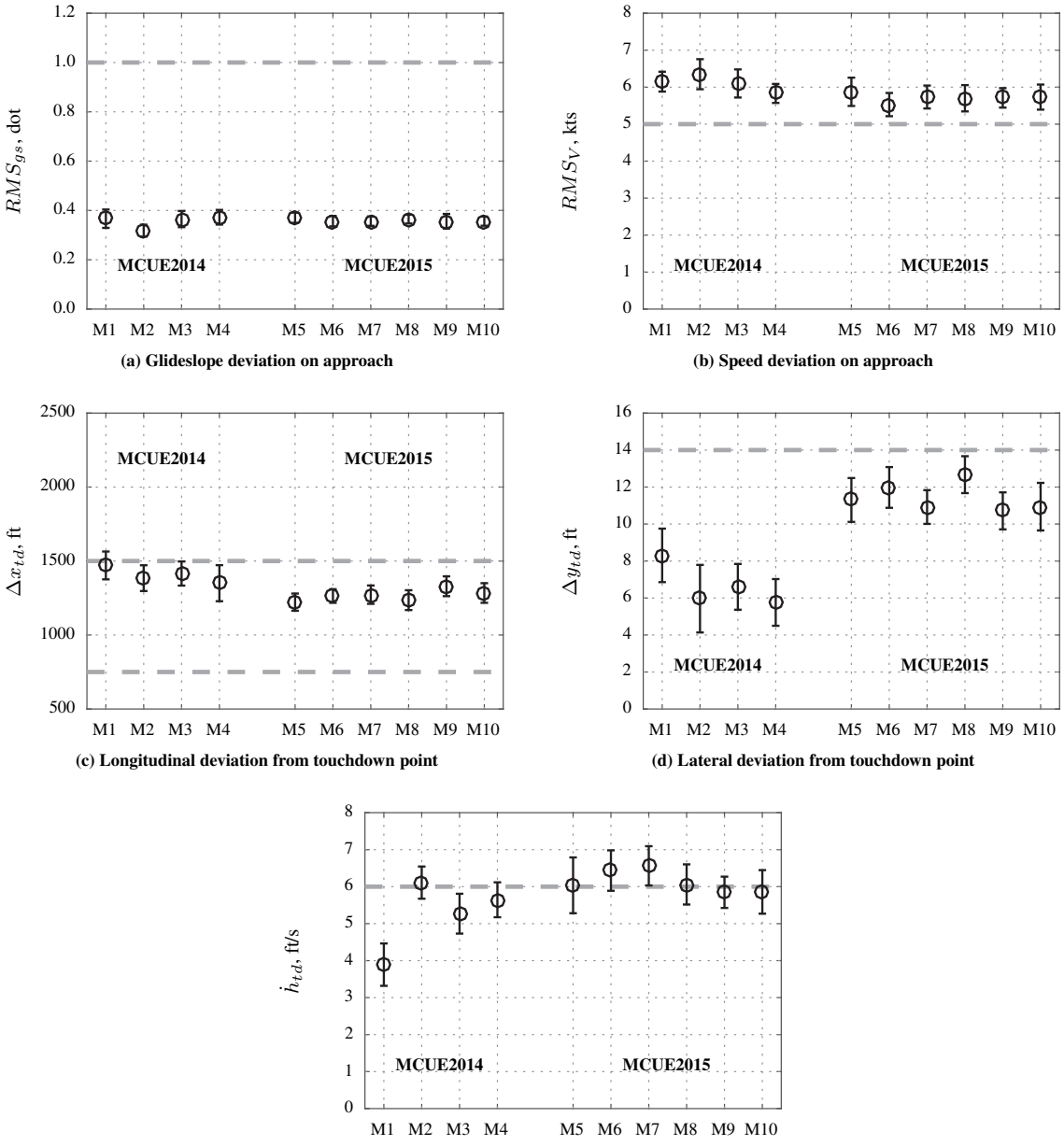

(a) Glideslope deviation on approach

(b) Speed deviation on approach

(c) Longitudinal deviation from touchdown point

(d) Lateral deviation from touchdown point

(e) Vertical speed at touchdown

Figure 11. Performance data of the approach and landing with sidestep task.

an average airspeed deviation between 5 and 6 kts. Pilots were slightly closer to meeting the speed-deviation requirement compared to the previous experiment.

The longitudinal and lateral deviations from the desired touchdown point were not significantly different between motion configurations (Figures 11c and 11d, respectively). Pilots generally touched down around the maximum allowable 1,500 ft from the runway threshold in the previous experiment; however, touched down well before the limit in the current experiment, around 1,250 ft. Pilots deviated much more laterally from the desired touchdown point in the current experiment compared to the previous experiment. The sink rate at touch down, depicted in Fig. 11e, was not statistically significantly different between motion configurations. The sink rate was around the maximum allowable value of 6 ft/s in every motion condition and very similar to the average sink rate in the hexapod motion configurations of the previous experiment (M2-M4).

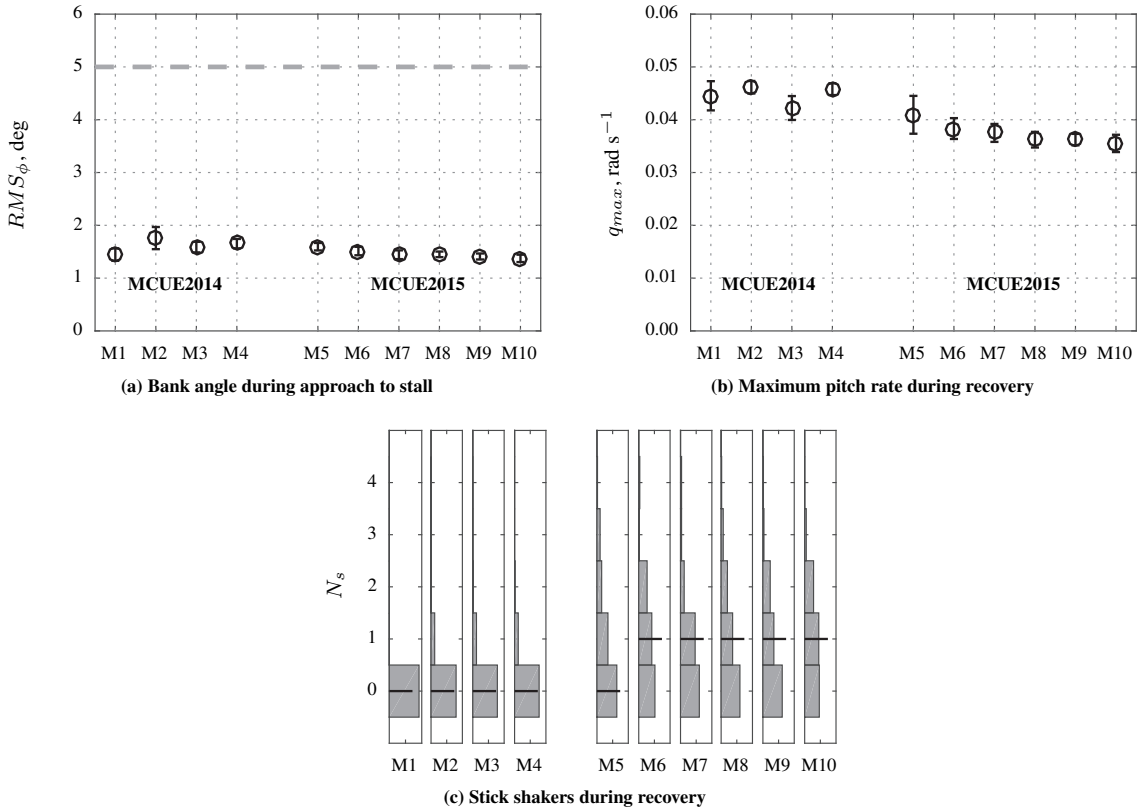

(a) Bank angle during approach to stall

(b) Maximum pitch rate during recovery

(c) Stick shakers during recovery

Figure 12. Performance data of the high altitude stall recovery task.

V.B.2. High-Altitude Stall Recovery Task

The task-performance results for the high-altitude stall recovery task are depicted in Fig. 12. The RMS roll deviation in the approach to the stall was significantly different between motion conditions and decreased going from M5 to M10 (Fig. 12a). Post-hoc analysis with Bonferroni adjustment revealed that the RMS roll deviation was significantly different between M5 and M8 ($p = 0.005$), M5 and M9 ($p = 0.003$), and M5 and M10 ($p = 0.050$). Note that pilots stayed well below the maximum allowable roll deviation in all conditions. Fig. 12b depicts the maximum pitch rate deviation during the stall recovery, which decreased from M5 to M10. The main ANOVA found that this variable was also significantly different between conditions. However, post-hoc analysis with Bonferroni adjustment revealed no significant differences between individual conditions.

The bars in Fig. 12c indicate the number of times a pilot activated 0, 1, 2, 3, or 4 additional stick shakers during the stall recovery. Medians of the data are depicted by the dashed horizontal lines. A Friedman test did not reveal any significant differences between conditions. Note that more additional stick shakers were triggered in the current experiment compared to the previous experiment. At most, two stick shakers were triggered in each condition of MCUE2014, while in some conditions of MCUE2015 up to four stick shakers were triggered.

V.B.3. Engine Out after Takeoff Task

Task performance for the engine out after takeoff task is depicted in Fig. 13. The RMS heading deviation after the engine failure was statistically significantly different between motion configurations and increasing from M5 to M10 (Fig. 13a). Post-hoc analysis with Bonferroni adjustment revealed that RMS heading deviation in condition M5 was significantly different from M7 ($p = 0.000$), M9 ($p = 0.003$), and M10 ($p = 0.006$), and marginally significantly different from M8 ($p = 0.099$). The RMS heading deviation in M6 was marginally significantly different from M7 ($p = 0.053$). When compared to the previous experiment, it can be observed that the RMS heading deviation in M5 was very similar to that in the large motion configuration M1. RMS heading deviation in M7 to M10 is very similar to that in the hexapod motion configurations of the previous experiment (M2-M4). Pilots were able to easily meet the heading performance criterion.

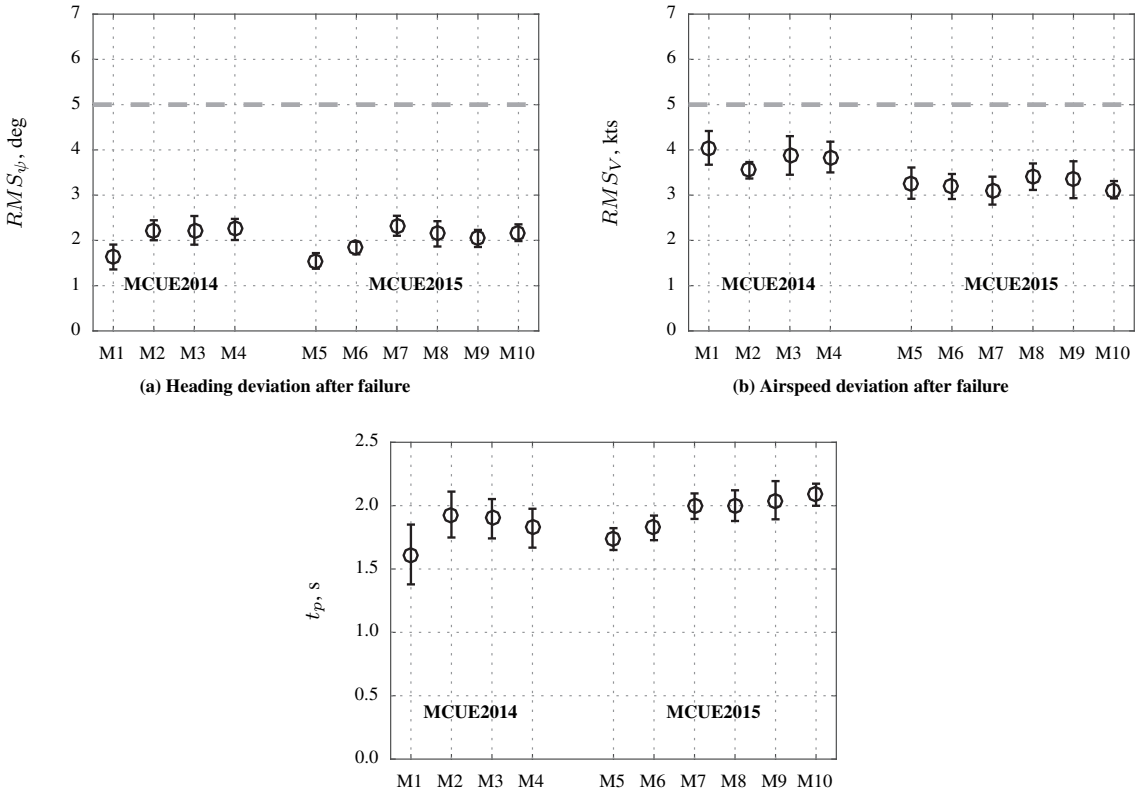

(a) Heading deviation after failure

(b) Airspeed deviation after failure

(c) Pedal input reaction time after failure

Figure 13. Performance data of the engine out on takeoff task.

The RMS speed deviation after the engine failure is depicted in Fig. 13b. The ANOVA did not detect any significant differences between motion configurations. The average RMS speed deviation appears to be lower compared to the previous experiment. Note that pilots were able to meet the speed performance criterion with ease. Fig. 13c depicts the reaction time of the initial pedal input after the engine failure. Significant differences between motion configurations were detected by the ANOVA. Post-hoc analysis revealed that the reaction time in M5 was statistically significantly different from M7 ($p = 0.039$), M8 ($p = 0.027$), M9 ($p = 0.028$), and M10 ($p = 0.001$). The reaction time in M6 was significantly different from M10 ($p = 0.006$). Note that the pedal reaction time follows a very similar pattern compared to the RMS heading deviation; that is, is increasing from M5 to M10. Values were comparable to the previous experiment.

V.C. False Motion Cues

In order to develop objective motion cueing criteria for the cross-coupling OMCT responses, the magnitude of false simulator motion cues due to cross coupling was determined in the sidestep and takeoff tasks. More specifically, the magnitude of false tilt cues due to insufficient turn coordination was determined in the approach with sidestep maneuver, while the magnitude of pitch rate due to tilt coordination was determined in the initial takeoff run.

During a coordinated turn in real flight, the lateral specific force due to roll is cancelled out by the lateral acceleration of the aircraft. However, in a simulator, limited lateral motion capabilities prevent this, resulting in a false lateral specific force that may be perceived by pilots as a tilting sensation. Jex et al. found that peak lateral specific forces with a magnitude above 0.1 g resulted in consistent pilot comments about false tilt cues.[11] Fig. 14a depicts the maximum lateral specific force due to roll in the aircraft body reference frame before reaching the decision altitude of 200 ft in the sidestep task. The dashed gray line indicates a specific force of 0.1 g. Note that the lateral specific forces in Fig. 14a are a result of the motion logic settings in the different motion configurations and also pilots' performance; that is, if roll angles remain smaller due to smaller wheel inputs in the sidestep maneuver, lateral specific forces remain smaller.

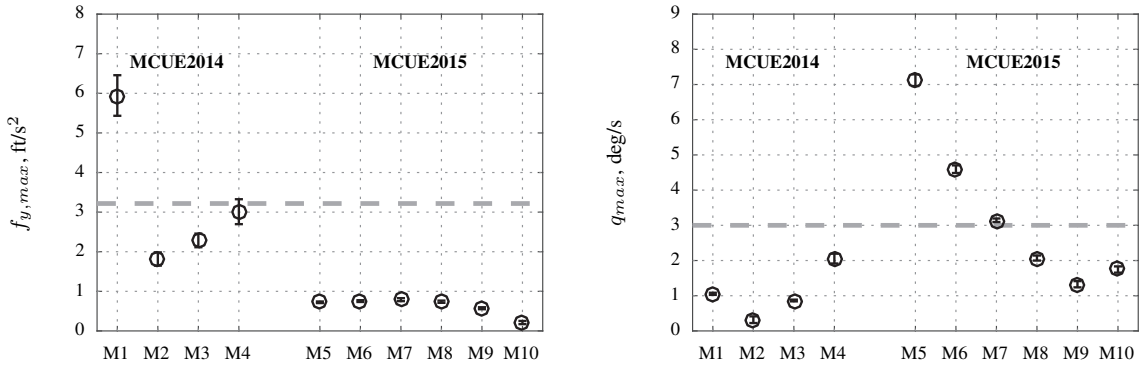

(a) Maximum lateral tilt cue **(b) Maximum tilt-coordination pitch rate**

Figure 14. False cues in the sidestep and takeoff tasks.

Fig. 14a shows that the maximum lateral specific forces due to roll stay well below the 0.1 g level for MCUE2015. For MCUE2014, the turn-coordination channel of the VMS motion logic was purposely turned off, resulting in much higher maximum lateral specific forces. The highest maximum lateral specific force due to roll is obtained for the full-motion condition M1. The maximum lateral specific force in condition M4 is just at the 0.1 g level.

Tilt coordination is the process of tilting the simulator cab to provide steady-state longitudinal and lateral accelerations at low frequencies. Groen et al. determined that whole-body tilt improves motion fidelity of visually simulated linear motion; however, rotational rates should not exceed approximately 3 deg/s.[20] Fig. 14b depicts the maximum pitch rate due to tilt coordination at the start of the takeoff roll. The dashed gray line indicates a rotational rate of 3 deg/s. Note that the rotational rates in Fig. 14b are also a combination of the motion logic settings in the different motion configurations and pilot inputs. The pitch rates remain smaller if the throttles are advanced more slowly.

The maximum pitch rate due to tilt coordination stays well below the 3 deg/s level for all conditions in MCUE2014. For MCUE2015, the maximum pitch rate due to tilt coordination is obtained for condition M5. The maximum pitch rate in condition M7 is approximately at the 3 deg/s level.

V.D. Objective Motion Cueing Criteria

Statistical differences in task performance between the motion configurations were used to refine the initial objective motion cueing criteria boundaries developed in the previous study. The same general procedure was followed as in Ref. 16. The ANOVA revealed that four dependent variables were statistically significantly different between motion configurations: the RMS roll deviation RMS_ϕ and the maximum pitch rate deviation q_{max} in the stall task, and the RMS heading deviation RMS_ψ and the pedal reaction time t_p in the takeoff task (see Table 2).

Fig. 15 shows the development of objective motion cueing criteria boundaries for the main OMCT responses based on the task performance results discussed above. The maximum pitch rate during the stall recovery was used to refine the pitch motion response criterion. No statistical differences between specific conditions were found for the maximum pitch rate in the post-hoc analysis with Bonferroni adjustment. Post-hoc analysis without adjustment for multiple comparisons revealed that M5 is significantly different from M8 ($p = 0.035$), M9 ($p = 0.022$), and M10 ($p = 0.032$). The motion responses of these motion conditions are depicted in Fig. 15a. The pitch response criterion boundary is defined by the smallest difference between the OMCT responses of M5 and any of the other motion conditions M8-M10. This criterion uncertainty boundary is the gray area in Fig. 15a. Note that task-performance differences between specific motion configurations were used to develop criteria in both the magnitude and phase plots. The RMS roll deviation in the stall task was used for the roll motion response criterion. Statistical differences were found between M5 and M8-M10. Hence, the OMCT responses of these motion conditions were used to define the roll motion response criterion equivalently to the pitch motion response criterion (Fig. 15b).

The RMS heading deviation and pedal reaction time in the takeoff task were used to determine the yaw and sway motion response criteria. Both dependent variables were statistically significantly affected in the same manner, and, therefore, the same motion configurations were used to develop both criteria. The yaw and sway motion response criteria boundaries, defined by the gray areas in Figures 16c and 16e, respectively, were defined by the smallest difference between the OMCT responses of M5 and any of the motion conditions M7-M10.

The objective motion cueing criteria boundaries for the cross-coupling OMCT responses were determined using the false-motion-cue analysis of Section V.C. Motion condition M4 in the sidestep task (MCUE2014) induced maximum lateral specific forces due to roll right at the human perception threshold for false tilt cues (Fig. 14a). The OMCT response of this motion condition was used to define the roll rate to lateral specific force motion response criterion. In motion condition M7, the maximum pitch rate due to tilt-coordination in the initial takeoff roll was right at the human perception threshold for rotational rate with a visual stimulus (Fig. 14b). The OMCT response of this motion configuration was used to define the longitudinal specific force to pitch rate motion response criterion.

Fig. 16 depicts the boundary uncertainties of the initial objective motion cueing criteria for the main motion responses. Both the boundaries developed in the first and the current experiments are depicted. One-to-one motion responses are also depicted in Fig. 16. Note that the new criteria boundaries are not overlapping the initial criteria boundaries over the entire frequency range. This might indicate that multiple boundaries are present and, for example, the initial boundaries developed in the previous experiment might divide the medium and high fidelity regions, while the new boundaries divide the low and medium fidelity regions.

Fig. 17 depicts the initial objective motion cueing criteria for the cross-coupling motion responses. These boundaries are developed using a single motion configuration, and, hence, no boundary uncertainties are present.

VI. Discussion

The experiment discussed in this paper is the third experiment in a project that aims to develop objective motion cueing criteria for commercial transport simulators. The first experiment was a quasi-transfer-of-training study evaluating whether different levels of training motion fidelity affect the initial training of commercial transport pilots.[21] This first study provided only a limited number of significant effects of the training motion, with some in the direction not predicted, possibly due to the fact that the general aviation pilots who participated in the study had no prior experience with the aircraft type used.

The second study did not focus on training, but on the effects of different levels of motion fidelity on pilots' performance in different flying tasks.[16] This experiment used experienced commercial airline transport pilots, representing pilots receiving recurrent training. More significant differences between motion configurations were found compared to the first experiment, and results were more in line with what was expected based on previous research. Based on the results from this second study, interim OMCT motion fidelity boundaries were proposed in Ref. 16. As only four motion configurations were tested, of which three were hexapod configurations and one was a large motion configuration, the motion fidelity boundaries had relatively large uncertainty margins. In addition, the boundaries were mostly situated in between the large motion and hexapod motion responses; that is, the motion fidelity boundaries defined a region of desired motion fidelity not achievable by hexapod simulators.

The purpose of the third experiment, discussed in this paper, was to refine the boundaries found in the previous experiment and explore more of the OMCT motion response region between the previously found boundary and the average OMCT response of a statistical sample of eight representative simulators. An additional goal was to develop initial criteria for the cross-coupling OMCT responses. The experiment used the same three tasks as the previous experiment with minor modifications; however, six new motion configurations were used.

Pilots used two motion ratings to rate the motion in two distinct parts of each task run. All ratings compared the simulator motion to real flight. No statistically significant differences were found across motion conditions in any of the motion ratings. It was hard for pilots to pay attention to the motion while performing the tasks and especially to remember the motion from earlier parts of the run. This might be one of the reasons pilots rated all runs similarly. In the sidestep task, no objective task performance measures were affected by the motion condition. Task performance was very similar to performance in the previous experiment; only the lateral deviation from the desired touchdown point was different. This difference is most likely caused by a change in turbulence characteristics between the two experiments.

Roll deviation in the approach to the stall and maximum pitch rate in the stall recovery were significantly affected by the motion condition in the stall task. From M5 to M10, the RMS of the roll angle and the maximum pitch rate decreased. Going from M5 to M10, the motion gains of the roll and pitch motion decreased; however, also the break frequencies of the washout filters decreased. This allowed for motion that helped more in keeping the roll angle in the approach to the stall at the desired value and helped with regulating pitch oscillations in the stall recovery, an effect typically observed in compensatory control tasks when the fidelity of motion feedback is increased.[10] The number of secondary stick shakers in the stall recovery was not significantly affected by motion in this experiment; however, was significantly higher compared to the previous experiment. This effect was most likely introduced by

minor adjustments in the calculation of the minimum speed at which the stick shaker is activated in this experiment compared to the previous experiment.

In the takeoff task, the RMS of the heading deviation and the reaction time of the initial pedal input after the engine failure were significantly affected by the motion condition. Both increased going from M5 to M7 and were approximately equal for M7-M10. This suggests that the increase in heading deviation is caused by pilots' delayed response to the engine failure as a result of lower fidelity motion cues. All takeoff task performance results for the current experiment were similar to the previous experiment. Note that the heading deviation and reaction time results for M5 and M6 are very similar tot the results from the large-motion condition M1. The results in conditions M7-M10 were very similar to the results from the hexapod motion conditions of the previous experiment (M2-M4). The RMS speed deviation after the engine failure seems slightly lower compared to the previous experiment. This might be the result of a slight modification of the force required to pull the nose up from the runway in this experiment compared to the previous experiment.

Summarizing, we found significant effects of motion on task performance for two of the three flight tasks. For the stall task we found better performance going from M5 to M10, and for the takeoff task going from M10 to M5. Overall, the biggest differences in performance were between M5 and M7/M8-M10. Based on these task performance results, OMCT motion fidelity boundaries were developed similarly to our previous experiment.[16] Motion fidelity boundaries were defined by first assigning a task performance result to each degree of freedom. Then, using significant differences in task performance between different motion configurations, fidelity boundaries were defined using the OMCT responses of those motion configurations. As the biggest differences in task performance were found between configurations M5 and M7/M8-M10, boundary uncertainties were defined by the smallest difference between the OMCT response of M5 and M7/M8-M10.

The goal of the current experiment was to refine the initial objective motion cueing criteria developed in the previous experiment. However, due to the nature of the motion configurations in the current experiment (covering the OMCT motion response region closer to what current hexapod simulators can achieve), the new motion fidelity uncertainty boundaries only partially intersect with the uncertainty boundaries found in the previous experiment. The question now arises if the new uncertainty boundaries are new boundaries dividing different fidelity regions compared to the boundaries found in the previous experiment, or if they are refinements of the previously found boundaries in the frequency range where they overlap. Furthermore, the RMS heading deviation and pedal reaction time in the takeoff task have been used to develop the motion criteria in both the sway and yaw degrees of freedom; however, motion in both or one of these degrees of freedom could have contributed to the significant differences found in task performance. In addition, we now assumed that significant differences in maximum pitch rate in the stall recovery were introduced by pitch motion; however, they could also have been introduced by the heave motion. The design of the motion configurations in the current experiment doesn't allow us to link motion in only one degree of freedom to one task performance result with absolute certainty.

In order to develop objective motion cueing criteria for the cross-coupling OMCT responses, false motion cues in the sidestep and takeoff tasks were analyzed. More precisely, the maximum lateral specific force due to roll in the sidestep turns and the pitch rate due to tilt coordination at the start of the takeoff roll were analyzed. Based on perception thresholds of these false motion cues taken from previous studies, objective motion cueing criteria for the roll-to-sway and surge-to-pitch responses were developed.[11,20] The perception thresholds used here were developed using dedicated tasks in highly controlled environments, and might not be accurate in the flying tasks used here. In the next experiment, we intend to use subjective motion ratings of false motion cues to refine the cross-coupling motion cueing criteria found in the current experiment.

Finally, the OMCT responses of the pitch, surge, and sway degrees of freedom include both low-pass characteristics from tilt-coordination and high-pass characteristics for the washout filters. The low-pass and high-pass response of different boundaries overlap, making it difficult to develop usable criteria for these degrees of freedom. A possible solution for this might be changing the OMCT such that only high-pass washout responses are included in the main OMCT responses. This will be explored further in future research.

Note again that the two darkest grey areas in Fig. 16 are believed to contain a motion fidelity boundary, but are not fidelity regions themselves like the light-grey fidelity regions developed in Ref. 3. The dark-grey areas are the regions of uncertainty for one side of a motion fidelity region. The other side of the region would be defined by the magnitude-of-one or zero-phase-error lines. Caution should be used when reducing the uncertainty of the initial fidelity boundaries developed in the previous study using the new boundary uncertainties from the current study, as they do not fully overlap. The next experiment will address the issues discussed in this section and aims to refine and optimize the fidelity boundaries further; that is, reduce the width of the dark-grey areas.

VII. Conclusions

This study used the Vertical Motion Simulator with three flight tasks and six different motion configurations per task to refine objective motion cueing criteria based on task performance developed in a previous study. The six motion configurations were designed to cover the OMCT motion response region between the motion criteria uncertainty boundaries found in the previous experiment and the mean OMCT response of a statistical sample of eight representative hexapod simulators. Fifteen experienced airline transport pilots participated, performing each task with all six motion configurations.

The experiment used both subjective and objective experimental measures. None of the subjective measures were significantly affected by the simulator motion condition, and no significant differences in task performance were found in the sidestep task. Task performance results in the stall task indicate that pilots deviated less from the desired roll angle in the motion conditions with a lower gain and lower washout break frequency. In the stall recovery, pilots had a lower maximum pitch rate in the conditions with a lower gain and lower break frequency. In the takeoff task, pilots deviated less from the desired heading and responded quicker after an engine failure in the motion conditions with higher motion gains.

Statistically significant differences in task performance found between the motion conditions were used to develop objective motion cueing fidelity boundaries. Further research is required to determine if these boundaries refine the initial boundaries from our previous experiment or if they represent new boundaries. Perception thresholds determined in previous research were used to develop initial criteria for the cross-coupling motion responses. Future experiments now underway will refine these boundaries further.

Acknowledgments

The authors thank the Vertical Motion Simulator simulation engineers who contributed to the experiment. We especially thank Nick Riccobono and Steve Norris for their valuable contributions in setting up and running the experiment. We also thank Colleen Cardoza for being our test pilot. Finally, we would like to thank Dr. Andrew Cheng from the FAA Technical Center for the continued program support.

References

[1]Code of Federal Regulations, *Flight Simulation Training Device Initial and Continuing Qualification and Use*, Title 14, Part 60.

[2]International Civil Aviation Organization, *ICAO 9625: Manual of Criteria for the Qualification of Flight Simulation Training Devices. Volume 1 – Aeroplanes*, 2009, 3rd edition.

[3]Hosman, R. J. A. W. and Advani, S. K., "Are Criteria for Motion Cueing and Time Delays Possible? Part 2." *Proceedings of the AIAA Modeling and Simulation Technologies Conference, Boston (MA)*, No. AIAA-2013-4833, 19–22 Aug. 2013.

[4]Sinacori, J. B., "The Determination of Some Requirements for a Helicopter Research Simulation Facility," Tech. Rep. NASA CR-152066, Systems Technology, Inc., Sept. 1977.

[5]Schroeder, J. A., "Helicopter Flight Simulation Motion Platform Requirements," Tech. Rep. NASA/TP-1999-208766, NASA, July 1999.

[6]Stapleford, R. L., Peters, R. A., and Alex, F. R., "Experiments and a Model for Pilot Dynamics with Visual and Motion Inputs," Tech. Rep. NASA CR-1325, NASA, 1969.

[7]Bergeron, H. P., Adams, J. J., and Hurt, Jr., G. J., "The Effects of Motion Cues and Motion Scaling on One- and Two-Axis Compensatory Control Tasks," NASA Technical Note NASA TN D-6110, NASA Langley Research Center, Jan. 1971.

[8]Bray, R. S., "Visual and Motion Cueing in Helicopter Simulation," Technical Memorandum NASA TM-86818, Ames Research Center, Moffett Field (CA), Sept. 1985.

[9]Cooper, D. E. and Howlett, J. J., "Ground Based Helicopter Simulation," *Proceedings of the American Helicopter Society Symposium on Status of Testing and Model Techniques for V/STOL Aircraft, Essington, PA*, 1973.

[10]Jex, H. R. and Magdaleno, R. E., "Roll Tracking Effects of G-vector Tilt and Various Types of Motion Washout," *Fourteenth Annual Conference on Manual Control*, University of Southern California, Los Angeles (CA), 25–27 April 1978, pp. 463–502.

[11]Jex, H. R., Jewell, W. F., and Magdaleno, R. E., "Effects of Various Lateral-Beam-Motion Washouts on Pilot Tracking and Opinion in the "Lamar" Simulator," *Fifteenth Annual Conference on Manual Control*, Wright State University, Dayton (OH), 20–22 March 1979, pp. 244–266.

[12]Bray, R. S., "Initial Operating Experience with an Aircraft Simulator Having Extensive Lateral Motion," Technical Memorandum NASA TM X-62,155, Ames Research Center, Moffett Field (CA), 1972.

[13]Bray, R. S., "Vertical Motion Requirements for Landing Simulation," Technical Memorandum NASA TM X-62,236, Ames Research Center, Moffett Field (CA), Feb. 1973.

[14]van Gool, M. F. C., "Influence of Motion Washout Filters on Pilot Tracking Performance," *Piloted Aircraft Environment Simulation Techniques*, No. AGARD-CP-249, AGARD, 1978, pp. 19–1 – 19–5.

[15]Shirachi, D. K. and Shirley, R. S., "Visual/Motion Cue Mismatch in a Coordinated Roll Maneuver," Contractor Report NASA CR-166259, Computer Sciences Corporation, Nov. 1981.

[16]Zaal, P. M. T., Schroeder, J. A., and Chung, W. W., "Objective Motion Cueing Criteria Investigation Based on Three Flight Tasks," *Proceedings of the Royal Aeronautical Society Flight Simulation Conference*, London, UK, 9–10 June 2015.

[17]Anonymous, *Military Specfication - Flying Qualities of Piloted Airplanes*, Department of Defence, U.S.A., Washington, D.C., Nov. 1980.

[18]Beard, S. D., Reardon, S. E., Tobias, E. L., and Aponso, B. L., "Simulation System Optimization for Rotorcraft Research on the Vertical Motion Simulator," *Proceedings of the AIAA Modeling and Simulation Technologies Conference, Minneapolis (MN)*, No. AIAA-2012-4634, 13–16 Aug. 2012.

[19]Field, A., *Discovering Statistics Using SPSS*, ISM Introducing Statistical Methods, SAGE Publications Ltd., 1 Oliver's Yard, 55 City Road, London EC1Y 1SP, 2nd ed., 2005.

[20]Groen, E. L. and Bles, W., "How to use body tilt for the simulation of linear self motion," *Journal of Vestibular Research*, Vol. 14, No. 5, Jan. 2004, pp. 375–385.

[21]Zaal, P. M. T., Schroeder, J. A., and Chung, W. W., "Transfer of Training on the Vertical Motion Simulator," *Journal of Aircraft*, Vol. 52, No. 6, Nov.–Dec. 2015, pp. 1971–1984.

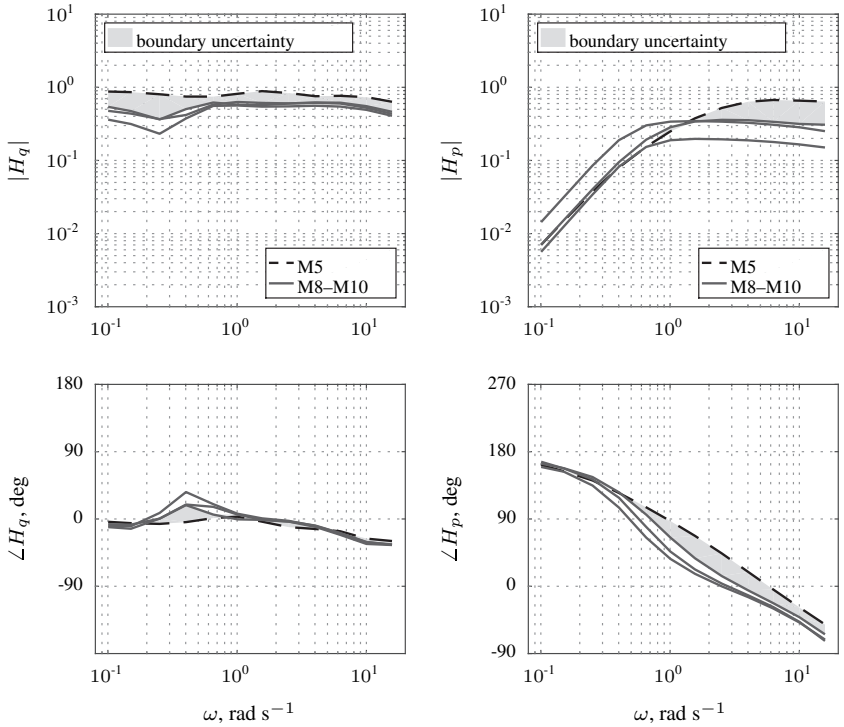

(a) Pitch response to pitch input.

(b) Roll response to roll input.

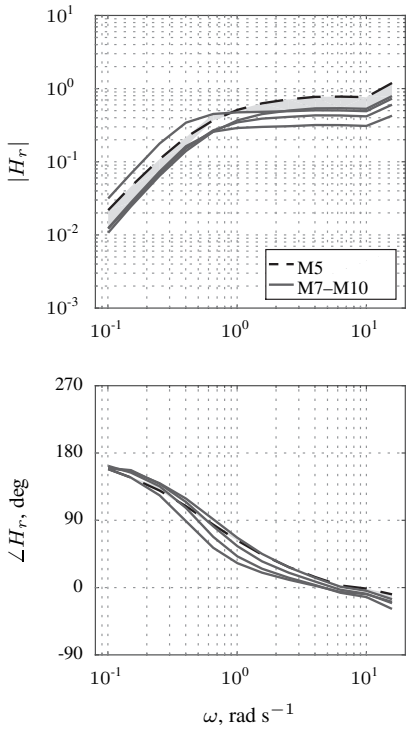

(c) Yaw response to yaw input.

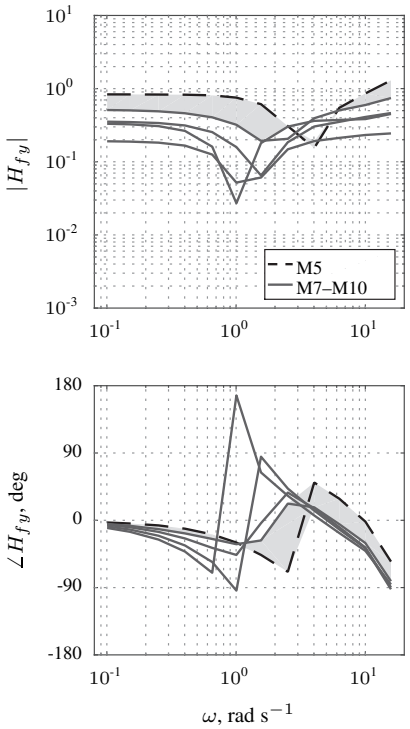

(d) Sway response to sway input.

Figure 15. Objective motion cueing criteria development.

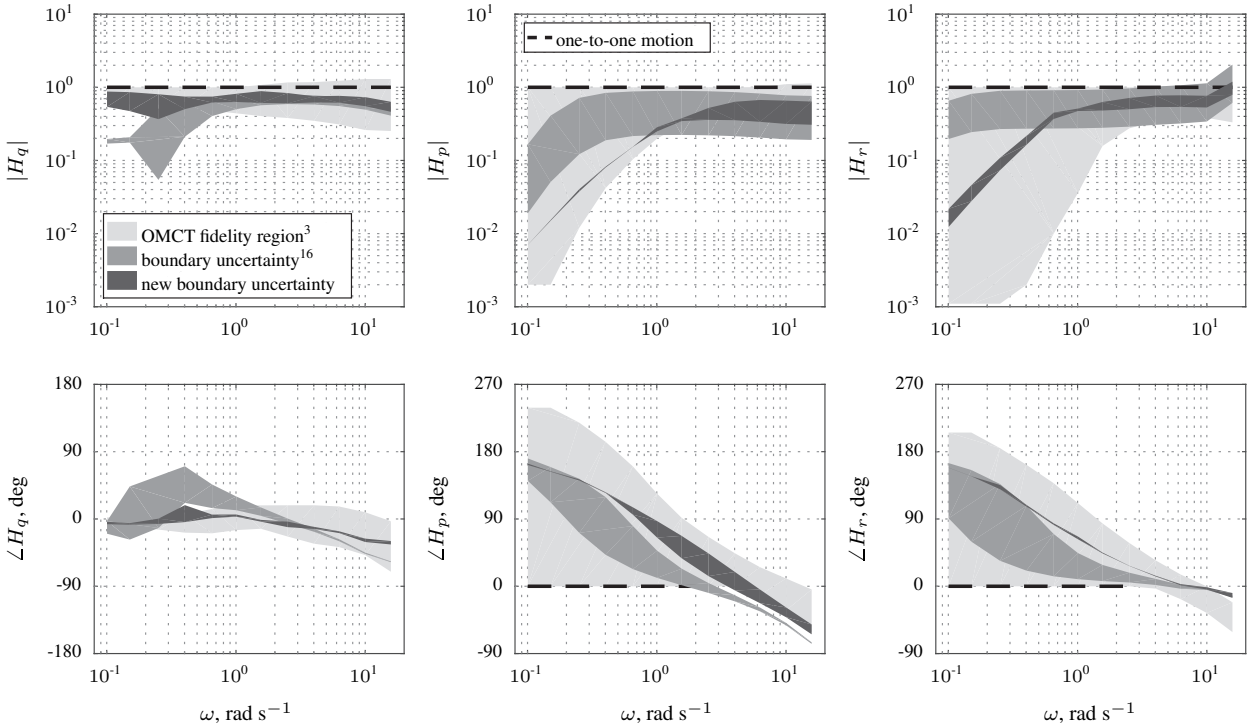

(a) Pitch response to pitch input. **(b) Roll response to roll input.** **(c) Yaw response to yaw input.**

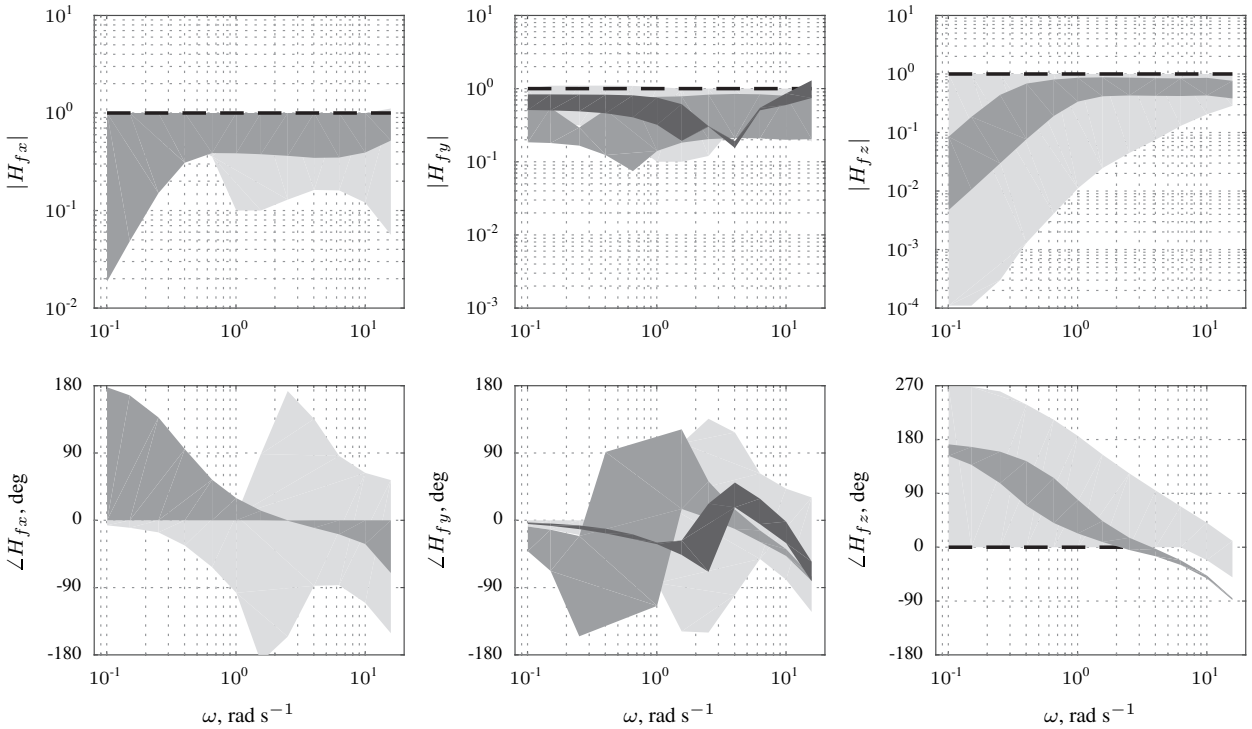

(d) Surge response to surge input. **(e) Sway response to sway input.** **(f) Heave response to heave inpput.**

Figure 16. Objective motion cueing criteria for the main OMCT responses.

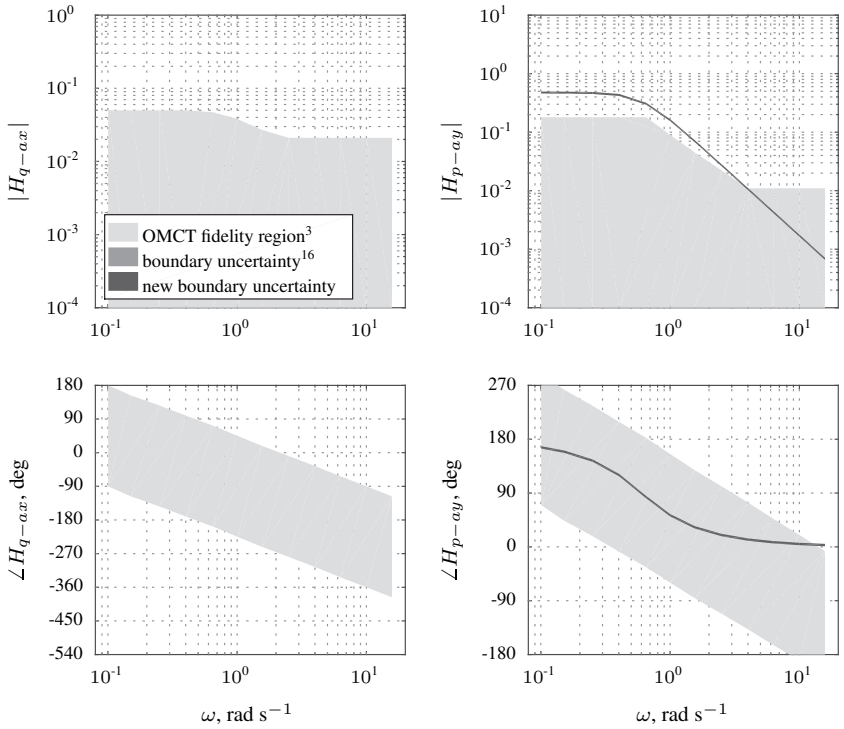

(a) Surge response to pitch input. **(b) Sway response to roll input.**

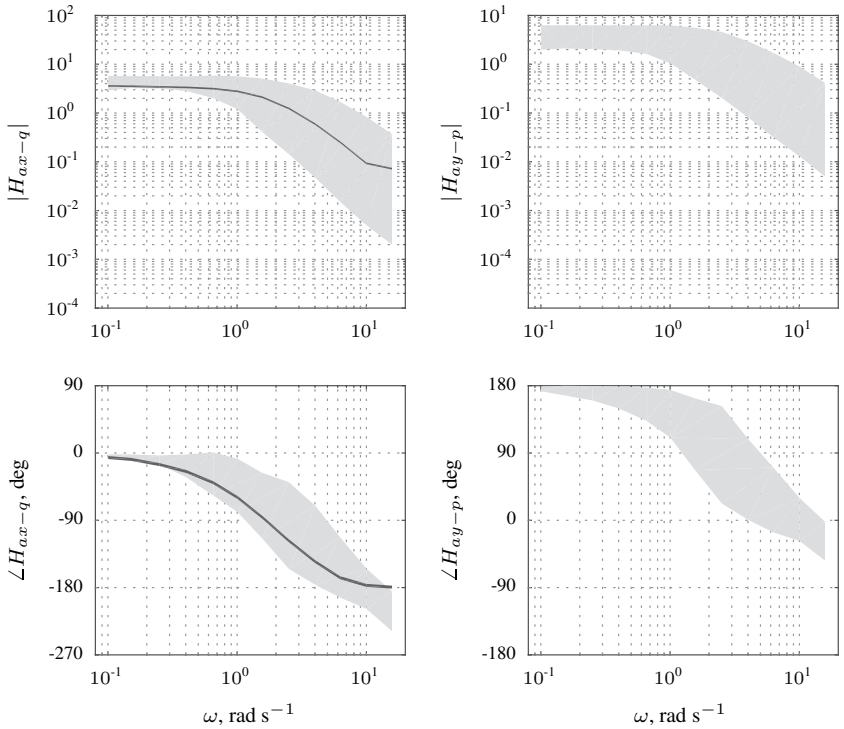

(c) Pitch response to surge input. **(d) Roll response to sway input.**

Figure 17. Objective motion cueing criteria for the cross-coupling OMCT responses.